High-risk plaque features can be detected in non-stenotic carotid plaques of patients with ischemic stroke classified as cryptogenic using combined FDG-PET/MR imaging

Fabien Hyafil*, MD, Ph.D [1-2]; Andreas Schindler*, MD [3]; Dominik Sepp*, MD [4]; Tilman Obenhuber, M.Sc. [3]; Anna Bayer-Karpinska, MD [5]; Tobias Boeckh-Behrens, MD [6]; Sabine Höhn [4]; Marcus Hacker, MD [7]; Stephan G. Nekolla, Ph.D [1-8]; Axel Rominger, MD [9]; Martin Dichgans, MD [4, 10]; Markus Schwaiger, MD [1]; Tobias Saam, MD [3]; Holger Poppert, MD [4].

[1] Department of Nuclear Medicine, Klinikum rechts der Isar, Technische Universität München, Munich, Germany; [2] Department of Nuclear Medicine, Bichat University Hospital, Inserm 1148, DHU FIRE, Assistance Publique – Hôpitaux de Paris, Paris, France; [3] Institute for Clinical Radiology, Ludwig-Maximilians-University Hospital Munich, Munich, Germany; [4] Department of Neurology, Klinikum rechts der Isar, Technische Universität München, Munich, Germany; [5] Institute for Stroke and Dementia Research, Ludwig-Maximilians-University Hospital Munich, Munich, Germany; [6] Department of Neuroradiology, Klinikum Rechts der Isar, Technische Universität München, Munich, Germany; [7] Division of Nuclear Medicine, Department of Biomedical Imaging and Image-guided Therapy, Medical, University of Vienna, Austria ; [8] German Centre for Cardiovascular Research (DZHK), Partner Site Munich Heart Alliance, Munich, Germany; [9] Department of Nuclear Medicine, Ludwig-Maximilians-University Hospital Munich, Munich, Germany ; [10] Munich Cluster of Systems Neurology (SyNergy), Munich, Germany.

* Contributed equally to this work

Word count: 5362

Corresponding Author:
Dr Fabien HYAFIL, MD, Ph.D.
Department of Nuclear Medicine, Klinikum rechts der Isar
Ismaninger Strasse 22, 81675 Munich, Germany
Email: fabien.hyafil@tum.de
Tel.: (+49) 89 4140 2965
Fax: (+49) 89 4140 4950

Abstract

Aims. High-resolution magnetic resonance imaging (MRI) can assess atherosclerotic plaque composition in carotid arteries with good correlation to histopathology. ^{18}Fluoro-deoxyglucose (FDG) is a positron emission tomography (PET) radiotracer that accumulates in inflammatory cells present in atherosclerotic plaques. The aim of this study was to investigate in 18 patients with ischemic stroke classified as cryptogenic and presenting non-stenotic carotid atherosclerotic plaques the morphological and biological aspects of these plaques with MRI and FDG-PET imaging.

Methods and Results. Carotid arteries were imaged 150 minutes after injection of FDG with a combined PET/MRI system. American Heart Association (AHA) lesion type and plaque composition were determined on consecutive MR axial sections (n = 460) in both carotid arteries. FDG uptake in carotid arteries was quantified using tissue-to-background ratio (TBR) on corresponding PET sections.

Prevalence of complicated atherosclerotic plaques (AHA type VI lesions) detected with high-resolution MRI was significantly higher in the carotid artery ipsilateral to the ischemic stroke as compared to the contralateral side (39% vs. 0 %; $p = 0.001$). For all other AHA lesion types, no significant differences were found between ipsilateral and contralateral sides. In addition, significantly higher FDG uptake was detected in advanced atherosclerotic plaques (AHA lesions ≥ type IV with high-resolution MRI) in the carotid artery ipsilateral to the stroke as compared with the contralateral artery (3.14 ± 1.13 vs. 2.44 ± 0.78, respectively; $p < 0.001$).

Conclusions. Morphological and biological features of high-risk plaques can be detected with high-resolution MRI and FDG-PET in non-stenotic atherosclerotic lesions ipsilateral to the stroke, supporting a causal role for these plaques in stroke.

Clinical Trial Registration. URL: https://clinicaltrials.gov; Unique Identifier: NCT01284933

Key words: atherosclerosis, vulnerable plaque, carotid arteries, stroke, MRI, PET, FDG.

Translational Perspective:

In 18 patients admitted for an ischemic stroke considered as cryptogenic, morphological and biological features of high-risk plaques were detected with high-resolution MRI and FDG-PET in non-stenotic atherosclerotic lesions ipsilateral to the stroke, supporting a causal role for these plaques in stroke. Furthermore, this study illustrates the potential value of combined PET/MRI systems for the more specific identification of high-risk carotid plaques.

Introduction

Stroke is one of the leading causes of death and handicap in industrialized countries (1, 2). Carotid plaques are estimated to cause between 15 and 20% of all ischemic strokes (3, 4). Plaque rupture is identified in about 60% of endarterectomy specimens of patients presenting with ischemic stroke and is thought to represent a key trigger for arterial thromboembolism (5). However, diagnostic and therapeutic strategies in patients with carotid stenosis remain based on the degree of luminal stenosis and the presence of acute ischemia in the downstream cerebral vascular territory (6). Detection of ruptured plaque with non-invasive imaging might help in identifying the origin of stroke or intermittent cerebral ischemia in symptomatic patients and in improving risk stratification in patients with asymptomatic carotid stenosis.

In the past 20 years, several non-invasive imaging techniques have demonstrated potential for the characterization of carotid atherosclerotic plaques (7, 8). Morphological plaque features such as thin/ruptured fibrous cap, large lipid-rich/necrotic core (LR/NC), or intraplaque hemorrhage (IPH) are characteristic of the so-called “high-risk plaque” and can be detected by high-resolution magnetic resonance imaging (MRI) with good accuracy in comparison with histology (9, 10). Additionally, carotid plaques of patients with recent ischemic stroke contain high numbers of inflammatory cells, which can be evidenced using ^{18}fluorodeoxyglucose (FDG), a glucose-analogue radiolabeled for positron emission tomography (PET) imaging that accumulates in metabolically active cells such as activated macrophages. Strong relationships have been documented between the degree of arterial FDG uptake and the density of macrophages determined histologically in carotid plaques (11). Moreover, atherosclerotic plaques of patients with carotid stenosis >50 % imaged shortly after transient ischemic attack accumulated approximately 30% more FDG in carotid arteries ipsilateral to the stroke than in contralateral arteries (12). Combined PET/MRI imaging systems (13) have recently become available and might prove particularly interesting for vascular

imaging by offering simultaneous morphological and functional evaluation of atherosclerotic plaques (14).

Non-stenotic carotid plaques represent a promising clinical application of plaque imaging. Indeed, in up to 40% of patients presenting with ischemic stroke despite extensive work-up, no definite cause can be established (15). In a first pilot study (16), we have imaged patients admitted for an ischemic stroke considered as cryptogenic and presenting non-stenotic carotid atherosclerotic plaques ipsilateral to the stroke with high-resolution multicontrast MRI. We found that about one-third of carotid plaques were complicated by intraplaque hemorrhage, fibrous plaque rupture, or luminal thrombus (AHA lesion type VI). Accurate identification of culprit atherosclerotic plaques associated with ischemic stroke is crucial because the prevalence of carotid stenosis <50% is high in the population. Histological analysis of plaques is, however, not available in these patients because most of the time they are treated medically. In the current study, we exploited the methodological opportunity of PET/MRI to simultaneously acquire structural and molecular signals in a subgroup of 18 patients included in the Carotid Plaque Imaging in Acute Stroke (CAPIAS) study (NCT01284933) (17) to identify specific features of high-risk carotid plaques.

Methods

Patient selection

Eighteen consecutive patients admitted to the stroke unit of the Department of Neurology of the University Hospital Klinikum rechts der Isar in Munich, Germany, between December 2012 and March 2014 were included in the CAPIAS study on the basis of previously published inclusion and exclusion criteria (17). Briefly, patients were screened for eligibility in the study on the basis of ischemic stroke in the territory of the anterior or middle cerebral artery < 14 days, non-stenosing atherosclerotic plaques in the carotid bifurcation determined by duplex sonography (plaque thickness > 2 mm; luminal stenosis < 50% according to North American Symptomatic Carotid Endarterectomy Trial criteria) and absence of any definite stroke etiology. The local ethics committee approved the study and all participants provided written informed consent.

Acquisition protocols with the combined PET-MRI system

Please see online supplemental data.

Analysis of FDG-PET and MR images of atherosclerotic plaques

Please see online supplemental data.

Statistical analysis

Categorical variables are presented as absolute and relative frequencies; continuous variables are presented as mean ± SD. For comparisons of ipsilateral and contralateral carotid arteries, paired Student's t-test was used to test differences between continuous variables, and Fisher's exact test, to determine differences between categorical variables. For comparisons of plaque composition in individual axial sections of carotid arteries, a two-sided Kruskall-Wallis test

was used to test differences between groups with continuous variables and heterogeneous variances. All analysis was performed using SAS version 9.2 (SAS Institute, Inc., Cary, North Carolina, USA). A p-value < 0.05 was considered statistically significant.

Results

Patient population

A total of 18 patients (mean age 70 ± 12 years; 37% male) with recent acute ischemic stroke and ipsilateral non-stenotic carotid atherosclerotic plaques were included in the study. Despite detailed clinical work-up, no definite stroke etiology was identified in any of these patients when they were included in this study. Demographic and clinical characteristics are described in Table 1. The mean Modified National Institute of Health Stroke Scale (NIHSS) (18) score upon admission was 3.5 ± 4.4. Average time between acute ischemic stroke and imaging was 6 ± 3 days. The average modified Rankin Scale and Barthel Index upon discharge was 1.7 ± 1.2 and 92 ± 14, respectively.

Morphology of carotid atherosclerotic plaques on multi-contrast MRI

A total of 460 out of 540 (85.2%) axial MR image sections were deemed interpretable. None of the patients had to be excluded due to poor image quality on MRI.

Quantitative analysis of plaque burden and composition (Table 2) identified no significant differences for mean luminal area or mean total vessel area between both carotid arteries. By contrast, significantly larger maximal wall areas were measured in the carotid artery ipsilateral to the stroke as compared with the contralateral artery. In addition, ipsilateral carotid arteries showed significantly larger maximum necrotic core and maximum hemorrhage areas than contralateral arteries. Maximum calcification areas did, however, not differ between ipsilateral and contralateral arteries.

Complicated atherosclerotic plaques (AHA type VI lesions) were detected in 39% (n = 7) of carotid arteries ipsilateral to the ischemic stroke (Table 2); by contrast, there were no AHA type VI plaque on the contralateral side (p = 0.001). For all other AHA lesion types, no significant differences were found between the ipsilateral and contralateral sides. The most common feature of AHA type VI lesions was intraplaque hemorrhage (100%), followed by fibrous plaque rupture (86%) and luminal thrombus (14%). Of the 7 arteries with intraplaque hemorrhage, 1 hemorrhage was classified as type I, and 6 were classified as type II.

FDG uptake in carotid arteries with PET

Relation between FDG uptake and plaque morphology

Increased FDG uptake was measured in ruptured atherosclerotic plaques and in plaques with a thin fibrous cap with MRI as compared with other lesions (Figure 1; TBR = 3.55 ± 1.21 and 3.14 ± 1.05 vs. 2.38 ± 0.83, respectively; $p < 0.001$). In addition, atherosclerotic plaques containing LR/NC or IPH with MRI (Figure 2) showed significantly higher FDG uptake as compared with other lesions (3.14 ± 1.14 vs. 2.36 ± 0.80 for the presence of a LR/NC; 3.48 ± 1.11 vs. 2.40 ± 0.84 for the presence of IPH; $p < 0.001$ each). Furthermore, plaques with large (≥ 5 mm^2) as compared with small (<5 mm^2) LR/NC were associated with higher FDG uptake (3.09 ± 1.04 vs. 2.58 ± 1.05, respectively; p = 0.001). Similarly, there was a strong trend for increased FDG uptake in plaques with large (≥ 5 mm^2) as compared with small (<5 mm^2) IPH type II, but this did not reach significance (3.76 ± 1.05 vs. 2.96 ± 0.71, respectively; p = 0.07). Atherosclerotic plaques classified as high-risk lesions with MRI (AHA lesions types IV/V and VI) were associated with higher FDG uptake in comparison with other AHA lesions (TBR = 3.09 ± 1.14 vs. 2.42 ± 0.82; respectively; $p < 0.001$).

When all axial sections of carotid arteries were selected, no significant difference in FDG uptake was detected between ipsilateral and contralateral carotid arteries (Figure 3; 2.55 ±

1.02 vs. 2.42 ± 0.83; p = 0.19). However, when only axial sections showing advanced atherosclerotic plaques (AHA lesion ≥ type IV with high-resolution MRI) were selected for analysis, significantly higher FDG uptake was detected in the carotid artery ipsilateral to the stroke as compared with the contralateral artery (3.14 ± 1.13 vs. 2.44 ± 0.78, respectively; p < 0.001).

AHA lesion type with MRI in sections with the highest FDG uptake with PET

In the axial section with the highest FDG uptake along both carotid arteries on PET (most-diseased segment), the prevalence of high-risk AHA lesions (types IV/V and VI) was 33%. Selecting only patients presenting high-risk or complicated carotid atherosclerotic plaques with MRI, the prevalence of high-risk AHA lesions (types IV/V and VI) increased to 50% in the section with the highest FDG uptake (Figure 4). Nevertheless, from the latter group of patients, 25% of sections with the highest FDG uptake along both carotid arteries with PET were composed only of small atherosclerotic plaques (AHA lesion type III) and 25% of sections had no plaque detectable (AHA lesion type I) on corresponding axial sections with high-resolution MRI (Figure 5).

Discussion

In this study, we evaluated in 18 consecutive patients with ischemic stroke classified as cryptogenic and presenting non-stenotic (<50%) carotid atherosclerotic plaques the morphological and biological aspects of these plaques using a combined PET/MRI system. We found that the prevalence of morphological features of high-risk atherosclerotic plaques on MRI was significantly higher in the carotid artery ipsilateral to the stroke than in the contralateral artery. In addition, carotid plaques presenting morphological features of high-risk plaques on MRI were associated with high levels of FDG uptake. Surprisingly, average

FDG uptake was similar in carotid arteries ipsilateral and contralateral to the stroke. In fact, we identified regions of carotid arteries with high FDG uptake with PET but exhibiting only minimal or no plaque with MRI. When only advanced atherosclerotic plaques identified with high-resolution MRI were selected for analysis, significantly higher FDG uptake was detected in the carotid artery ipsilateral to the stroke than in the contralateral artery. These observations highlight the value of combined PET-MRI systems for the more specific identification of high FDG uptake originating from increased inflammatory activity present in complicated carotid plaques.

Role of combined PET-MRI systems for the evaluation of carotid plaques

In this study, we first confirmed that non-stenotic carotid atherosclerotic plaques of patients with recent ischemic stroke have morphological features of plaque instability as well as high levels of inflammatory activities (i.e., FDG uptake) similar to what has been previously observed non-invasively and histologically in stenotic plaques. In a previous study (19), the association between high-risk morphological features of plaques with computed tomographic angiography (CTA) and high FDG uptake has been described in patients with carotid stenosis >50%. However, characterization of plaques with CTA is limited to the detection of surface irregularities and areas of hypodensities. In this study, we took advantage of spatial and temporal co-registration provided by simultaneous PET/MR imaging to confirm that morphological features associated with plaque instability identified with high-resolution MRI such as fibrous cap rupture, large LR/NC, and IPH were also associated with high FDG uptake.

An important diagnostic question remains what the incremental role of FDG-PET over high-resolution MRI is for the evaluation of non-stenotic atherosclerotic plaques (20). Interestingly, both the intensity of inflammation measured on histology (21) and the presence

of high FDG uptake detected with PET (22) in atherosclerotic plaques have recently been shown to be independent predictors of early stroke recurrence in patients with carotid stenosis >50%. In a similar way, we postulate that FDG-PET might, in addition to MRI, improve risk stratification of symptomatic patients with non-stenotic plaques and help to identify patients who could benefit from early interventional approaches. This hypothesis will need to be evaluated prospectively in a larger group of patients.

Role of combined PET/MRI in therapeutic studies

Vascular FDG-PET imaging is increasingly being used as surrogate marker for the evaluation of new drugs aimed at plaque stabilization (23). The rationale for including FDG-PET imaging in clinical studies is that the decrease in FDG uptake in the vessel wall can appear as early as 3 months after introduction of therapies (24, 25) and has been associated with later regression of plaque volume (26). In order to sensitize the detection of potent drug effects, the current proposed strategy for clinical trials is to measure changes in the intensity of FDG uptake in areas of the vessel wall showing the highest uptake of radiotracer on the initial PET acquisition (26, 27). In this study, we have provided evidence that regions with the highest FDG signal along carotid arteries may be associated with only small plaques (AHA lesion type III) or no plaque (AHA lesion type I) on corresponding high-resolution MRI. In fact, in this study of a cohort of symptomatic patients, we show that areas with the highest FDG uptake with PET contain at best only 50% of high-risk atherosclerotic plaques on corresponding MRI. Perivascular FDG uptake has previously been described in patients with stenotic carotid plaques using PET/CT acquisitions and identified as a cause of discrepancies between FDG uptake and the intensity of macrophage infiltration measured on corresponding histological sections (19). We speculate that this perivascular FDG uptake might originate from the presence of small immune structures developing in the vessel wall independently of

intimal composition. Combined PET/MRI systems might therefore be helpful in clinical studies to identify FDG uptake associated with advanced plaques and, hence, to evaluate more accurately the effects of drugs on inflammatory activities in atherosclerotic plaques.

Limitations

This study requires several reservations. First, the results of the present study are limited by the modest sample size, but its strength lies in the simultaneous assessment of FDG activity and plaque morphology by high-resolution PET/MRI. We took advantage of this combined image acquisition to evaluate the relationship between well-validated plaque characteristics detected with high-resolution MRI and the intensity of FDG uptake. Second, PET axial sections were reconstructed with a slice thickness of 2 mm to allow for optimal matching with MR images. The true spatial resolution of PET images is in the range 4 to 5 mm. The intensity of FDG uptake measured on each axial section with PET might therefore be partly influenced by signal originating from adjacent sections of atherosclerotic plaques. Finally, only symptomatic patients with non-stenotic carotid plaques were imaged in this study. Morphological and functional characteristics of plaques in this group of patients evaluated by the association of high-resolution MRI and FDG-PET will need to be compared with the aspects observed in a cohort of asymptomatic patients in order to identify the most accurate imaging criteria associated with high-risk carotid plaques.

Conclusions

This work demonstrates that, in patients admitted for an ischemic stroke considered as cryptogenic, non-stenotic atherosclerotic plaques ipsilateral to the stroke presented morphological and biological features of complicated plaques with high-resolution MRI and FDG-PET, supporting a causal role for these plaques in stroke. In addition, simultaneous

identification of advanced carotid plaques with high-resolution MRI in association to PET imaging allowed for the more accurate detection of FDG uptake related to inflammation in plaques. Accordingly, combined PET/MRI might have a role in the future for risk stratification of carotid plaques as well as in assessing more specifically the therapeutic effects of novel therapies aimed at plaque stabilization on inflammatory cells present in atherosclerotic plaques.

Acknowledgments

We thank Sylvia Schachoff, Anna Winter, and Claudia Meisinger for their valuable help in acquiring PET/MR images in the patients of this study and Isabelle Dregelly for setting up MR sequences.

Funding sources

This work was supported by the European Research Advanced Grant "Multimodal Molecular Imaging" and by the German Research foundation DFG (Deutsche Forschungsgemeinschaft, Grossgeräteinitiative), which funded the installation of the PET/MRI system.

Disclosures

Markus Schwaiger has a research cooperation contract with Siemens Healthcare AG. No other potential conflict of interest relevant to this article was reported.

References

1. Go AS, Mozaffarian D, Roger VL, Benjamin EJ, Berry JD, Blaha MJ, Dai S, Ford ES, Fox CS, Franco S, Fullerton HJ, Gillespie C, Hailpern SM, Heit JA, Howard VJ, Huffman MD, Judd SE, Kissela BM, Kittner SJ, Lackland DT, Lichtman JH, Lisabeth LD, Mackey RH, Magid DJ, Marcus GM, Marelli A, Matchar DB, McGuire DK, Mohler ER, 3rd, Moy CS, Mussolino ME, Neumar RW, Nichol G, Pandey DK, Paynter NP, Reeves MJ, Sorlie PD, Stein J, Towfighi A, Turan TN, Virani SS, Wong ND, Woo D, Turner MB, American Heart Association Statistics C, Stroke Statistics S. Heart disease and stroke statistics--2014 update: a report from the American Heart Association. Circulation. 2014;**129**:e28-e292.

2. Krishnamurthi RV, Feigin VL, Forouzanfar MH, Mensah GA, Connor M, Bennett DA, Moran AE, Sacco RL, Anderson LM, Truelsen T, O'Donnell M, Venketasubramanian N, Barker-Collo S, Lawes CM, Wang W, Shinohara Y, Witt E, Ezzati M, Naghavi M, Murray C, Global Burden of Diseases IRFS, the GBDSEG. Global and regional burden of first-ever ischaemic and haemorrhagic stroke during 1990-2010: findings from the Global Burden of Disease Study 2010. The Lancet Global health. 2013;**1**:e259-81.

3. Bonita R. Epidemiology of stroke. Lancet. 1992;**339**:342-4.

4. Risk of stroke in the distribution of an asymptomatic carotid artery. The European Carotid Surgery Trialists Collaborative Group. Lancet. 1995;**345**:209-12.

5. Redgrave JN, Lovett JK, Gallagher PJ, Rothwell PM. Histological assessment of 526 symptomatic carotid plaques in relation to the nature and timing of ischemic symptoms: the Oxford plaque study. Circulation. 2006;**113**:2320-8.

6. Adams RJ, Albers G, Alberts MJ, Benavente O, Furie K, Goldstein LB, Gorelick P, Halperin J, Harbaugh R, Johnston SC, Katzan I, Kelly-Hayes M, Kenton EJ, Marks M, Sacco RL, Schwamm LH, American Heart A, American Stroke A. Update to the AHA/ASA recommendations for the prevention of stroke in patients with stroke and transient ischemic attack. Stroke. 2008;**39**:1647-52.

7. Naghavi M, Libby P, Falk E, Casscells SW, Litovsky S, Rumberger J, Badimon JJ, Stefanadis C, Moreno P, Pasterkamp G, Fayad Z, Stone PH, Waxman S, Raggi P, Madjid M, Zarrabi A, Burke A, Yuan C, Fitzgerald PJ, Siscovick DS, de Korte CL, Aikawa M, Airaksinen KE, Assmann G, Becker CR, Chesebro JH, Farb A, Galis ZS, Jackson C, Jang IK, Koenig W, Lodder RA, March K, Demirovic J, Navab M, Priori SG, Rekhter MD, Bahr R, Grundy SM, Mehran R, Colombo A, Boerwinkle E, Ballantyne C, Insull W, Jr., Schwartz RS, Vogel R, Serruys PW, Hansson GK, Faxon DP, Kaul S, Drexler H, Greenland P, Muller JE, Virmani R, Ridker PM, Zipes DP, Shah PK, Willerson JT. From vulnerable plaque to vulnerable patient: a call for new definitions and risk assessment strategies: Part II. Circulation. 2003;**108**:1772-8.

8. Rudd JH, Hyafil F, Fayad ZA. Inflammation imaging in atherosclerosis. Arterioscler Thromb Vasc Biol. 2009;**29**:1009-16.

9. Yuan C, Mitsumori LM, Beach KW, Maravilla KR. Carotid atherosclerotic plaque: Noninvasive MR characterization and identification of vulnerable lesions. Radiology. 2001;**221**:285-99.

10. Yuan C, Mitsumori LM, Ferguson MS, Polissar NL, Echelard D, Ortiz G, Small R, Davies JW, Kerwin WS, Hatsukami TS. In vivo accuracy of multispectral magnetic resonance imaging for identifying lipid-rich necrotic cores and intraplaque hemorrhage in advanced human carotid plaques. Circulation. 2001;**104**:2051-6.

11. Tawakol A, Migrino RQ, Bashian GG, Bedri S, Vermylen D, Cury RC, Yates D, LaMuraglia GM, Furie K, Houser S, Gewirtz H, Muller JE, Brady TJ, Fischman AJ. In vivo 18F-fluorodeoxyglucose positron emission tomography imaging provides a noninvasive measure of carotid plaque inflammation in patients. J Am Coll Cardiol. 2006;**48**:1818-24.

12. Rudd JH, Warburton EA, Fryer TD, Jones HA, Clark JC, Antoun N, Johnstrom P, Davenport AP, Kirkpatrick PJ, Arch BN, Pickard JD, Weissberg PL. Imaging atherosclerotic plaque inflammation with [18F]-fluorodeoxyglucose positron emission tomography. Circulation. 2002;**105**:2708-11.

13. Judenhofer MS, Wehrl HF, Newport DF, Catana C, Siegel SB, Becker M, Thielscher A, Kneilling M, Lichy MP, Eichner M, Klingel K, Reischl G, Widmaier S, Rocken M, Nutt RE, Machulla HJ, Uludag K, Cherry SR, Claussen CD, Pichler BJ. Simultaneous PET-MRI: a new approach for functional and morphological imaging. Nature Medicine. 2008;**14**:459-65.

14. Rischpler C, Nekolla SG, Beer AJ. PET/MR imaging of atherosclerosis: initial experience and outlook. American Journal of Nuclear Medicine and Molecular Imaging. 2013;**3**:393-6.

15. Amarenco P. Underlying pathology of stroke of unknown cause (cryptogenic stroke). Cerebrovascular diseases. 2009;**27**:97-103.

16. Freilinger TM, Schindler A, Schmidt C, Grimm J, Cyran C, Schwarz F, Bamberg F, Linn J, Reiser M, Yuan C, Nikolaou K, Dichgans M, Saam T. Prevalence of nonstenosing, complicated atherosclerotic plaques in cryptogenic stroke. JACC Cardiovasc Imaging. 2012;**5**:397-405.

17. Bayer-Karpinska A, Schwarz F, Wollenweber FA, Poppert H, Boeckh-Behrens T, Becker A, Clevert DA, Nikolaou K, Opherk C, Dichgans M, Saam T. The carotid plaque imaging in acute stroke (CAPIAS) study: protocol and initial baseline data. BMC Neurology. 2013;**13**:201.

18. Meyer BC, Hemmen TM, Jackson CM, Lyden PD. Modified National Institutes of Health Stroke Scale for use in stroke clinical trials: prospective reliability and validity. Stroke. 2002;**33**:1261-6.

19. Figueroa AL, Subramanian SS, Cury RC, Truong QA, Gardecki JA, Tearney GJ, Hoffmann U, Brady TJ, Tawakol A. Distribution of inflammation within carotid atherosclerotic plaques with high-risk morphological features: a comparison between positron emission tomography activity, plaque morphology, and histopathology. Circ Cardiovasc Imaging. 2012;**5**:69-77.

20. Rominger A, Saam T, Wolpers S, Cyran CC, Schmidt M, Foerster S, Nikolaou K, Reiser MF, Bartenstein P, Hacker M. 18F-FDG PET/CT identifies patients at risk for future vascular events in an otherwise asymptomatic cohort with neoplastic disease. J Nucl Med. 2009;**50**:1611-20.

21. Marnane M, Prendeville S, McDonnell C, Noone I, Barry M, Crowe M, Mulligan N, Kelly PJ. Plaque inflammation and unstable morphology are associated with early stroke recurrence in symptomatic carotid stenosis. Stroke. 2014;**45**:801-6.

22. Marnane M, Merwick A, Sheehan OC, Hannon N, Foran P, Grant T, Dolan E, Moroney J, Murphy S, O'Rourke K, O'Malley K, O'Donohoe M, McDonnell C, Noone I, Barry M, Crowe M, Kavanagh E, O'Connell M, Kelly PJ. Carotid plaque inflammation on 18F-fluorodeoxyglucose positron emission tomography predicts early stroke recurrence. Annals of Neurology. 2012;**71**:709-18.

23. Hyafil F, Feldman L, Le Guludec D, Fayad ZA. Evaluating efficacy of pharmaceutical interventions in atherosclerosis: role of magnetic resonance imaging and positron emission tomography. The Mount Sinai Journal of Medicine. 2012;**79**:689-704.

24. Tahara N, Kai H, Ishibashi M, Nakaura H, Kaida H, Baba K, Hayabuchi N, Imaizumi T. Simvastatin attenuates plaque inflammation: evaluation by fluorodeoxyglucose positron emission tomography. J Am Coll Cardiol. 2006;**48**:1825-31.

25. Tawakol A, Fayad ZA, Mogg R, Alon A, Klimas MT, Dansky H, Subramanian SS, Abdelbaky A, Rudd JH, Farkouh ME, Nunes IO, Beals CR, Shankar SS. Intensification of statin therapy results in a rapid reduction in atherosclerotic inflammation: results of a multicenter fluorodeoxyglucose-positron emission tomography/computed tomography feasibility study. J Am Coll Cardiol. 2013;**62**:909-17.

26. Fayad ZA, Mani V, Woodward M, Kallend D, Abt M, Burgess T, Fuster V, Ballantyne CM, Stein EA, Tardif JC, Rudd JH, Farkouh ME, Tawakol A, dal PI. Safety and efficacy of dalcetrapib on atherosclerotic disease using novel non-invasive multimodality imaging (dal-PLAQUE): a randomised clinical trial. Lancet. 2011;**378**:1547-59.

27. Elkhawad M, Rudd JH, Sarov-Blat L, Cai G, Wells R, Davies LC, Collier DJ, Marber MS, Choudhury RP, Fayad ZA, Tawakol A, Gleeson FV, Lepore JJ, Davis B, Willette RN, Wilkinson IB, Sprecher DL, Cheriyan J. Effects of p38 mitogen-activated protein kinase inhibition on vascular and systemic inflammation in patients with atherosclerosis. JACC Cardiovasc Imaging. 2012;**5**:911-22.

Figure legends

Figure 1. Relationship between morphological features of high-risk atherosclerotic plaques with MRI and the intensity of FDG uptake with PET. Significantly higher FDG uptake was measured in ruptured atherosclerotic plaques or in plaques with a thin fibrous cap on MRI as compared with other lesions. In addition, atherosclerotic plaques containing lipid-rich necrotic core (LR/NC) or intraplaque hemorrhage (IPH) with MRI showed significantly higher FDG uptake as compared with lesions lacking these morphological features. Furthermore, plaques with large (≥5 mm^2) as compared with small (< 5mm^2) LR/NC were associated with higher FDG uptake. Similarly, there was a strong trend for increased FDG uptake in plaques with large (≥5 mm^2) as compared with small (<5 mm^2) IPH type II, but this did not reach significance. Furthermore, atherosclerotic plaques classified as high-risk on MRI (AHA lesions types IV/V and VI) were associated with higher FDG uptake in comparison with other AHA lesions. *, $p < 0.05$. †, $p = 0.07$.

Figure 2. Representative example of high-risk carotid atherosclerotic plaque formed of lipid-rich/necrotic core and intraplaque hemorrhage imaged with combined FDG-PET/MRI. Corresponding axial views of non-stenotic carotid atherosclerotic plaque acquired simultaneously using a combined imaging system including magnetic resonance imaging (MRI) with successive high-resolution black-blood T2-weighted (A), black-blood T1-weighted before (B) and 5 minutes after injection of gadolinium chelates (C) and time-of-flight (TOF; D) sequences, and positron emission tomography (PET) images (E) acquired 150 minutes after injection of ^{18}fluorodeoxyglucose (FDG) allowing for perfect matching of both acquisitions (F; fusion image formed of TOF and FDG-PET images). Note the presence of a non-stenotic atherosclerotic plaque ipsilateral to the vascular territory of the stroke (A–D; white arrowhead) formed of a hypointense area on T1-, and T2-weighted and TOF sequences

and a hyperintense area on T1-, and T2-weighted and TOF sequences consistent with the presence of a lipid-rich necrotic core associated with intraplaque hemorrhage type II. High accumulation of FDG was detected with PET in the corresponding area (E–F; white arrowhead), supporting the presence of high inflammatory activity in the atherosclerotic plaque.

Figure 3. AHA lesion types with high-resolution MRI corresponding to the most-diseased segment identified with FDG-PET imaging. In axial sections with the highest FDG uptake detected with PET, the prevalence of high-risk AHA lesions (types IV/V and VI) was measured at 33.3%. When only the subgroup of patients presenting vulnerable or complicated carotid plaques with MRI was selected for analysis, the prevalence of high-risk AHA lesions (types IV/V and VI) increased to 50%. However, in the latter group, 25% of axial sections were composed of small atherosclerotic plaques (AHA lesion type III) and 25% of sections had no plaque detectable (AHA lesion type I) on corresponding high-resolution MRI.

Figure 4. Intensity of FDG uptake measured with PET in carotid atherosclerotic plaques. When all axial sections of carotid arteries were selected, no significant difference in FDG uptake was detected between ipsilateral and contralateral carotid arteries. When only axial sections showing advanced atherosclerotic plaques (AHA lesion ≥ type IV) with high-resolution MRI were selected for analysis, significantly higher FDG uptake was detected in the carotid artery ipsilateral to the stroke as compared with the contralateral artery. *, $p = 0.19$; †, $p < 0.05$

Figure 5. Representative example of axial section with the highest FDG uptake along the carotid artery with PET demonstrating absence of any plaque detectable on corresponding MRI. Corresponding axial views of carotid arteries acquired simultaneously using a combined PET-MR imaging system with successive high-resolution black-blood T2-weighted (B), black-blood T1-weighted before (C) and 5 minutes after injection of gadolinium chelates (D) and time-of-flight (TOF; D) sequences, and positron emission tomography images (E, PET; F, fusion image formed of TOF and FDG-PET images). No plaque or lymph node can be detected with MR sequences in the area presenting the highest FDG uptake along both carotid arteries with PET (white arrow; A–F).

Table 1. Patient population.

	n	%
Vascular risk factors/comorbidities		
Active smoking	3	17
Former smoking	10	56
Diabetes mellitus	4	22
Hypercholesterolemia	5	28
Arterial hypertension	13	72
Positive family history for vascular events	10	56
Overweight (body mass index > 25 kg/m^2)	12	67
Coronary artery disease	4	22
Periphery arterial disease	2	11
Baseline medications		
Antiplatelet agent plus statin	4	22
Statin only	2	11
Antiplatelet agent only	3	17
Neither antiplatelet agent nor statin	9	50

Table 2. Plaque characteristics with MRI ipsilateral and contralateral to the vascular territory of ischemic stroke.

	Ipsilateral side (n = 18)	**Contralateral side (n = 18)**	**p-value**
Plaque burden			
Mean total vessel area (mm^2)	58.1	55.9	0.34
Mean lumen area (mm^2)	28.7	31.5	0.33
Maximal wall area (mm^2)	47.8	37.2	0.003
Plaque composition (mm^2)			
Maximal lipid core area	11.3	1.6	< 0.001
Maximal hemorrhage area	0.5	0.0	0.02
Maximal calcified area	0.6	1.2	0.21
AHA lesion type distribution			
Type VI	7 (39 %)	0 (0 %)	0.008
Intra-plaque hemorrhage	7 (39 %)	0 (0 %)	0.008
Fibrous cap rupture	6 (33 %)	0 (0 %)	0.002
Thrombus	1 (6 %)	0 (0 %)	1
Type I	2 (11 %)	2 (11 %)	1
Type III	4 (22 %)	8 (44 %)	0.31
Type IV/V	2 (11 %)	3 (17 %)	0.63
Thin fibrous cap	1 (6 %)	0 (0 %)	1
Thick fibrous cap	1 (6%)	3 (17 %)	0.60
Type VI	7 (39 %)	0 (0 %)	0.008
Type VII	3 (17 %)	5 (28 %)	0.69
Type VIII	0 (0 %)	0 (0 %)	1

Figure 1

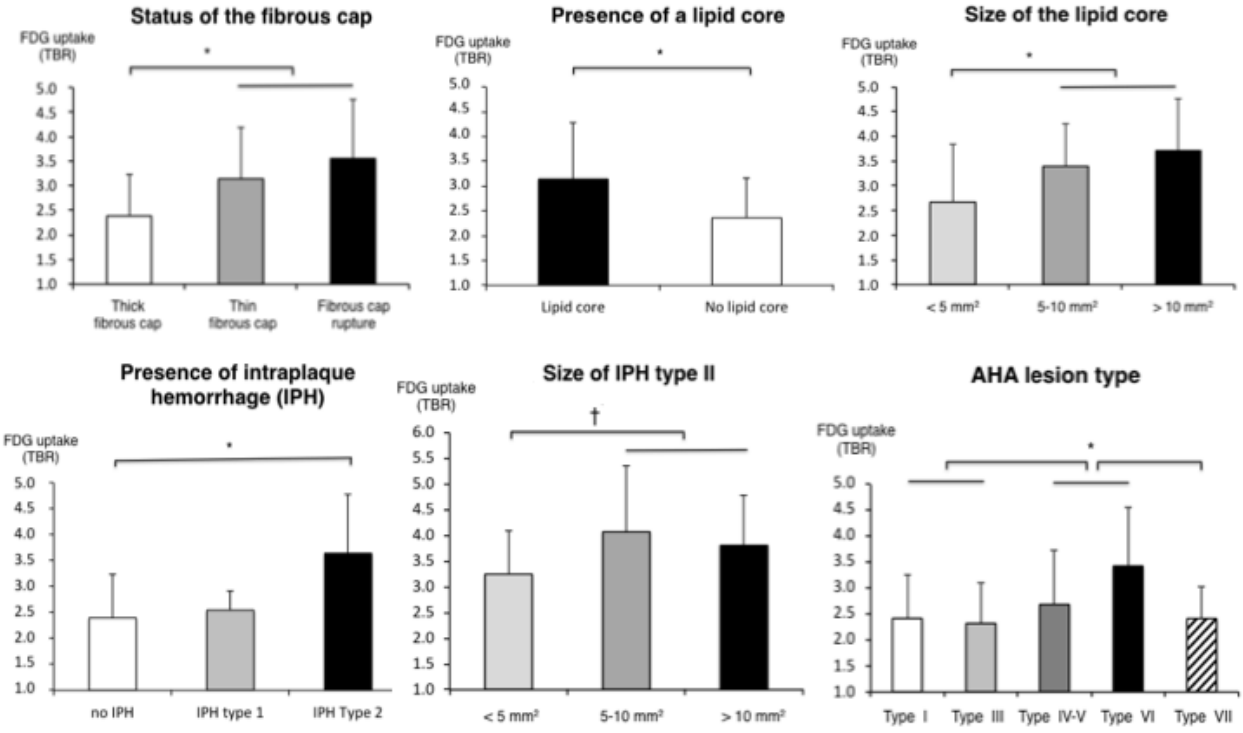
Status of the fibrous cap
FDG uptake (TBR)
Thick fibrous cap
Thin fibrous cap
Fibrous cap rupture
Presence of a lipid core
Lipid core
No lipid core
Size of the lipid core
< 5 mm²
5-10 mm²
> 10 mm²
Presence of intraplaque hemorrhage (IPH)
no IPH
IPH type 1
IPH Type 2
Size of IPH type II
AHA lesion type
Type I
Type III
Type IV-V
Type VI
Type VII

Figure 2

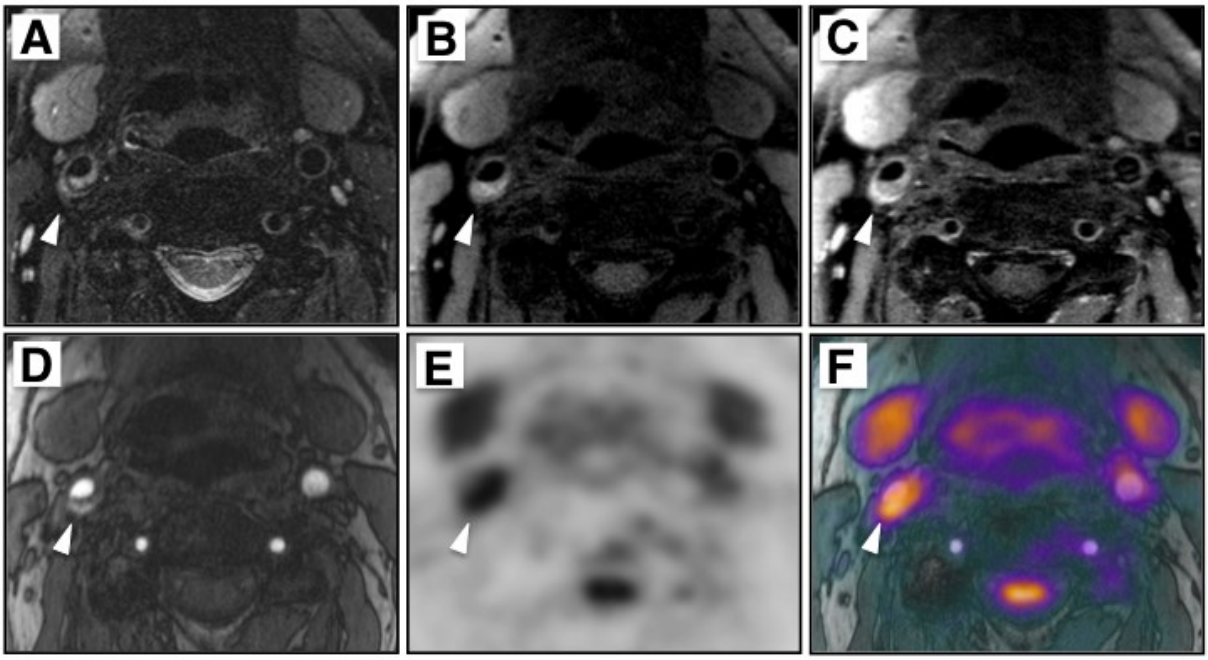

Figure 3.

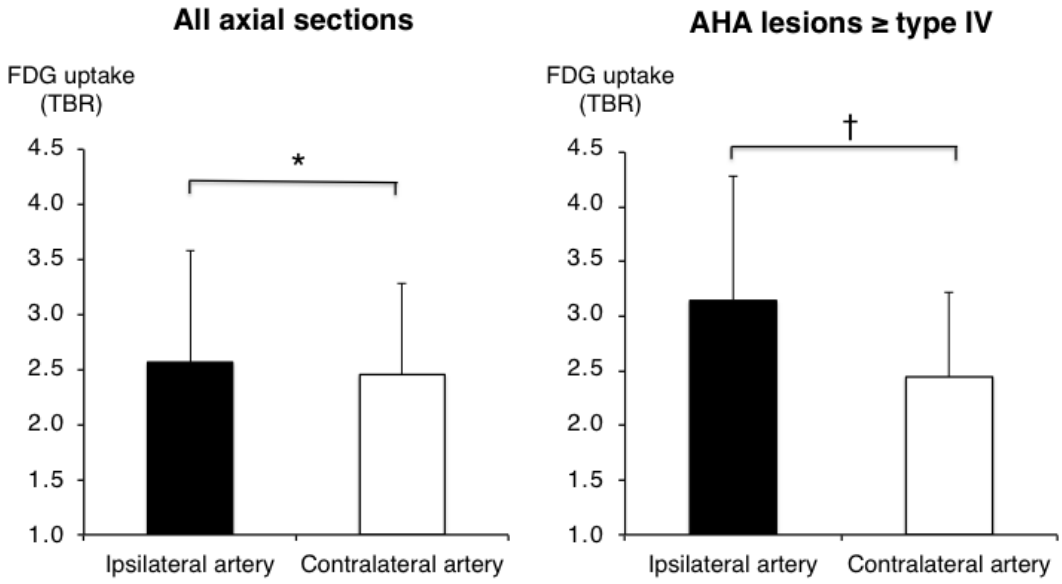
All axial sections
FDG uptake
(TBR)
4.5
4.0
3.5
3.0
2.5
2.0
1.5
1.0
*
Ipsilateral artery
Contralateral artery
AHA lesions ≥ type IV
FDG uptake
(TBR)
4.5
4.0
3.5
3.0
2.5
2.0
1.5
1.0
†
Ipsilateral artery
Contralateral artery

Figure 4.

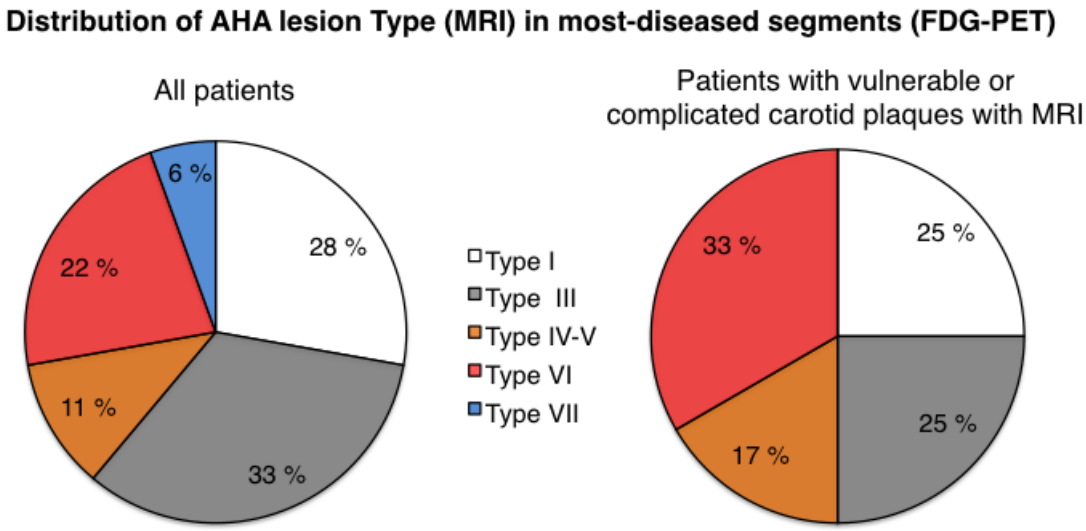
Distribution of AHA lesion Type (MRI) in most-diseased segments (FDG-PET)
All patients
6 %
28 %
22 %
11 %
33 %
Type I
Type III
Type IV-V
Type VI
Type VII
Patients with vulnerable or complicated carotid plaques with MRI
33 %
25 %
25 %
17 %

Figure 5